Effects of Dead Load and Multiple Earthquake Loadings on Seismic Performance of Wood-Frame Shear Walls

Kevin B. D. White
Thomas H. Miller
Rakesh Gupta

Abstract

Goals of this preliminary study are to better understand (1) earthquake performance of wood-frame shear walls carrying gravity loads, compared with walls without gravity load, and (2) performance of walls subjected to a sequence of earthquake motions, compared with walls subjected to a single earthquake.

Tests with simulated earthquake ground motions were conducted on 2,440 by 2,440-mm (8 by 8-ft) walls with 38 by 89-mm (nominal 2 by 4) Douglas-fir studs at 610 mm (24 in.) on center. Two oriented strand board (OSB) panels were installed and fastened vertically to the frame, and two gypsum wallboard panels were installed opposite the OSB. Partially anchored (PA) walls had two anchor bolts on the sill plate. In addition to the anchor bolts, fully anchored (FA) walls included hold-downs installed at the end studs. Ground motions were scaled to the 10 percent in 50 years probability of exceedance design level for Seattle, Washington, the traditional level associated with life safety performance.

For PA walls with dead load, failure modes were consistent with tests without dead load; however, additional fastener damage, common to FA walls, resulted from the additional resistance to overturning. PA walls realized a greater improvement in performance from dead load application compared with FA walls; performance appears to approach that of FA walls when dead load is applied. FA and PA walls subjected to a sequence of earthquake motions showed wall performance about the same as that of walls subjected to a single scaled earthquake motion.

Earthquakes are relatively common in the Pacific Northwest. According to the Pacific Northwest Seismograph Network (2005), each year several thousand earthquakes are recorded, although only a few dozen are large enough to be felt. Lateral loads imposed upon buildings from these earthquakes, and also as a result of wind, are random and cyclic, and these loads are resisted by the building's lateral force resisting system (LFRS). The Portland Cement Association (1997) reported that more than 90 percent of US residences have shear walls as their primary LFRS. Usually, shear walls resist lateral loads and also provide support to the weight (or gravity load) of the structure above; however, shear wall design capacities are most often based on tests that do not account for the vertical load. A research program was therefore developed to better understand shear wall behavior under realistic loading conditions. The objectives of this study were the following:

1. To evaluate earthquake performance of residential shear walls, following provisions of the International Residential Code (IRC) (International Code Council [ICC] 2006) carrying gravity loads, and to compare the results with those of walls carrying no gravity loads. These walls have only anchor bolts and no hold-downs.
2. To evaluate residential shear wall performance when subjected to a sequence of earthquakes, and to compare the results with those of walls subjected to a single earthquake ground motion.

The authors are, respectively, former Graduate Research Assistant, Dept. of Wood Sci. and Engineering (kevin.white.is@gmail.com), Associate Professor, School of Civil and Construction Engineering (thomas.miller@oregonstate.edu), and Professor, Dept. of Wood Sci. and Engineering (rakesh.gupta@oregonstate.edu), Oregon State Univ., Corvallis. This paper was received for publication in July 2009. Article no. 10663.

Forest Prod. J. 60(2):150–156.

Literature Review

To date, there has been limited experimental study to evaluate the effect of vertical load on wood shear wall performance. Dujic and Zarnic (2001) conducted monotonic and quasi-static cyclic tests with 2.4 by 2.4-m (8 by 8-ft) oriented strand board (OSB)–sheathed fully anchored (FA) and partially anchored (PA) walls. Vertical loads of 4.17 kN/m (286 lb/ft), 21.25 kN/m (1,456 lb/ft), and 35 kN/m (2,400 lb/ft) were used to represent the vertical load on walls in the fifth, third, and first story, respectively. For walls carrying the smallest vertical load, hold-downs increased the racking resistance. For walls carrying more than 20 kN/m (1,370 lb/ft), hold-downs had very little effect on lateral resistance of the wall. The conclusion was that walls carrying small vertical loads should be anchored with hold-downs, and that vertical load improves the racking strength of walls. Yanaga et al. (2002) conducted a numerical study on FA and PA walls carrying dead load. They determined that PA walls carrying sufficient dead load have strength similar to that of FA walls that are not carrying dead load. They also observed that PA walls have much lower strength and displacement capacity when dead loads are not applied. Ni and Karacabeyli (2002) investigated the performance of PA and FA shear walls subjected to either static loading or reverse cycling (International Organization for Standardization 1998). In addition, some walls were vertically loaded. Various magnitudes of vertical load were used: 4.6 kN/m (315 lb/ft), 9.1 kN/m (624 lb/ft), 13.7 kN/m (939 lb/ft), and 18.2 kN/m (1,247 lb/ft). They observed that aspect ratio and vertical load magnitude influenced the capacity of PA walls. PA wall capacity was similar to that of FA walls when sufficient vertical load was applied. If vertical load was not present, PA walls achieved 50 percent of the capacity of FA walls with vertical load. In general, the rate of increase in capacity decreased with increasing vertical load.

Seaders (2004) conducted two monotonic tests using PA walls that had different applied gravity loads (4.39 kN/m [301 lb/ft] and 7.30 kN/m [500 lb/ft]). Seaders observed that the increase in load-carrying capacity was related to the magnitude of the dead load resisting moment. Seaders then suggested that FA walls may represent an upper bound to increases resulting from dead load application, although it is unlikely that this upper limit will be reached just by adding vertical load to PA walls because of P-Δ moment amplification effects. He et al. (1998) conducted cyclic tests using the Forintec Canada Corporation (FCC), European Committee for Standardization (CEN)–short, and CEN-long protocols with 7.2 by 2.4-m (24 by 8-ft) walls carrying a 9.12-kN/m (625-lb/ft) gravity load. However, no tests were conducted without vertical load, so an analysis of the effect of vertical load was not performed. Karacabeyli and Ceccotti (1996, 1998) and Ni et al. (1999) summarized a shear wall testing program conducted by the Forintek Canada Corporation. Although numerous wall treatments, test protocols, and vertical loads were compared, the effect of vertical load was not discussed. Likewise, Durham et al. (1998) conducted monotonic and cyclic tests as well as tests using the 1992 Landers, California, ground motion. Shear walls anchored with conventional hold-downs and sheathed with standard or oversized OSB panels were used. All walls were subjected to a gravity load of 9 kN/m (617 lb/ft) to represent the weight of one story. Unfortunately, the effect of the vertical load could not be completely determined. Nonetheless, they observed that for shorter walls, the gravity load was crucial to resist uplift at wall corners.

Limited research has been reported on shear walls subjected to a sequence of earthquake ground motions, or a sequence of many test protocols, although some of the standard cyclic test protocols were developed with the intention of representing multiple earthquakes. Durham et al. (2001) tested 2.4 by 2.4-m (8 by 8-ft) FA walls, sheathed with large, 2.4 by 2.4-m (8 by 8-ft) OSB panels. The objectives were to determine the advantages, if any, of using large OSB panels. One test, scaled to a peak ground acceleration (PGA) of 0.35*g,* did not damage the wall. Thus, the wall was tested again using a PGA of 0.52*g*. The second test severely damaged the sheathing-to-frame connections, causing nails to pull through the sheathing, nail fracture, and complete nail withdrawal. After these two successive tests, researchers decided to repair the damaged wall and perform a third test with a PGA of 0.3*g*. Results of the third test indicate that the wall was more flexible and had a lower capacity; however, it performed similar to walls sheathed with one horizontally oriented 1.2 by 2.4-m (4 by 8-ft) panel along the bottom of the wall and two 1.2 by 1.2-m (4 by 4-ft) panels at the top of the wall. Researchers concluded that a severely damaged wall can be retrofitted to achieve reasonable performance. McMullin and Merrick (2000) conducted a sequence of force-controlled cyclic tests on FA walls sheathed with plywood, OSB, or gypsum wallboard (GWB) on both sides. One test, with GWB sheathing only, exhibited no visible damage after 20 load cycles. Thus, a second test with double the load was conducted; the wall failed after just a few cycles. Total energy dissipated from this two test sequence was 2.3 times greater than for the nonsequence test of walls sheathed with plywood. These studies by McMullin and Merrick (2000) involved further testing as a result of incomplete wall failure during the initial test. Furthermore, the walls were nonconventionally sheathed, and only one wall was tested sequentially per study. Additional research is needed to determine wall performance during a sequence of earthquake ground motions or other load types.

Materials and Methods

Wall specimens and anchorage

Tests with earthquake ground motions were conducted on 2,440 by 2,440-mm (8 by 8-ft) walls with Standard and Better 38 by 89-mm (nominal 2 by 4) Douglas-fir studs 610 mm (24 in.) on center. The walls were constructed in accordance with the IRC (ICC 2006)–prescribed braced panel construction. Two 1,220 by 2,440 by 11.1-mm (4 ft by 8 ft by 7/16-in.) 24/16 American Plywood Association (APA)–rated OSB panels were installed and fastened vertically to the frame with 8d nails (2.87 by 60.33 mm [0.113 by 2.375 in.]) at 152 mm (6 in.) and 305 mm (12 in.) on center along panel edges and intermediate studs, respectively. Two 12.7-mm (0.5-in.) GWB panels were also installed vertically on the frame face opposite to that of the OSB with bugle head wallboard screws (2.31 by 41.3 mm [0.09 by 1.63 in.]) spaced 305 mm (12 in.) on center along the panel edges and intermediate studs. The GWB was used to most closely simulate actual shear walls in residential construction. PA walls had two 12.7-mm (0.5-in.) A307 anchor bolts installed 305 mm (12 in.) inward on the sill plate from each end of the wall. In addition to anchor bolts,

FA walls included hold-downs installed at the end studs of the wall attached to the foundation with 15.9-mm (⅝-in.) Grade 5 anchor bolts.

Test frame and equipment

As described in White et al. (2009), the test frame consisted of a 102 by 152 by 10-mm (4 by 6 by 0.4-in.) steel beam on linear bearings at each end. Two 51-mm (2-in.) solid steel rods rigidly attached to the strong floor of the laboratory were guides for the bearings. A 4.45-kN (1-kip) servo-controlled hydraulic actuator capable of 153 mm (6 in.) of stroke drove the steel load beam horizontally in one dimension to simulate ground motions. Walls were connected to the moveable steel beam serving as a foundation. Shear walls in buildings laterally support the mass of all components tributary to them from the structure above. Here, a 4,543-kg (10,000-lb) tributary mass was used for a typical shear wall in a 140-m^2 (1,500-ft^2) residential home. For safety, seismic mass was placed on a steel cart rolling on the floor and connected to the top of the wall. The cart rested on steel tracks rigidly attached to the strong-floor of the laboratory and also connected to the bottom end of the moment arm by a steel rod pinned at both ends. The steel channel bolted to the top of the walls was laterally braced to a strong-wall in the laboratory through a series of steel struts. This limited movement of the top of the wall to the one dimension in which the wall was being driven by the hydraulic actuator.

The frame was modified to apply a controlled vertical load to the test walls, as depicted in Figure 1. To apply a vertical load, a 4.8-mm-diameter (0.19-in.-diameter) steel cable was run through a series of pulleys and attached to the steel load beam at 0.61 m (2 ft) in from each end of the wall. The cable was attached to a 25.4-mm (1-in.) hydraulic cylinder with a 355-mm (14-in.) stroke, which applied the load. This setup yielded a 2:1 mechanical advantage and applied ½ of the total vertical load (5.35 kN [1.20 kips]) at 0.61 m (24 in.) in from each end of the wall. Note that the vertical load on the wall and the tributary mass for lateral loading are not the same, because nonbraced walls in the house support gravity loads. A 4.45-kN (1-kip) load cell was installed in-line with the cable to provide feedback to a Continental Hydraulics analog control board with proportional gain so that gravity load could be monitored and controlled to help in maintaining gravity load during dynamic lateral loading. Note that some additional inaccuracies are present: the P-Δ effect of the gravity load is not simulated with this system, and cable rotation may lead to minor lateral loads as well.

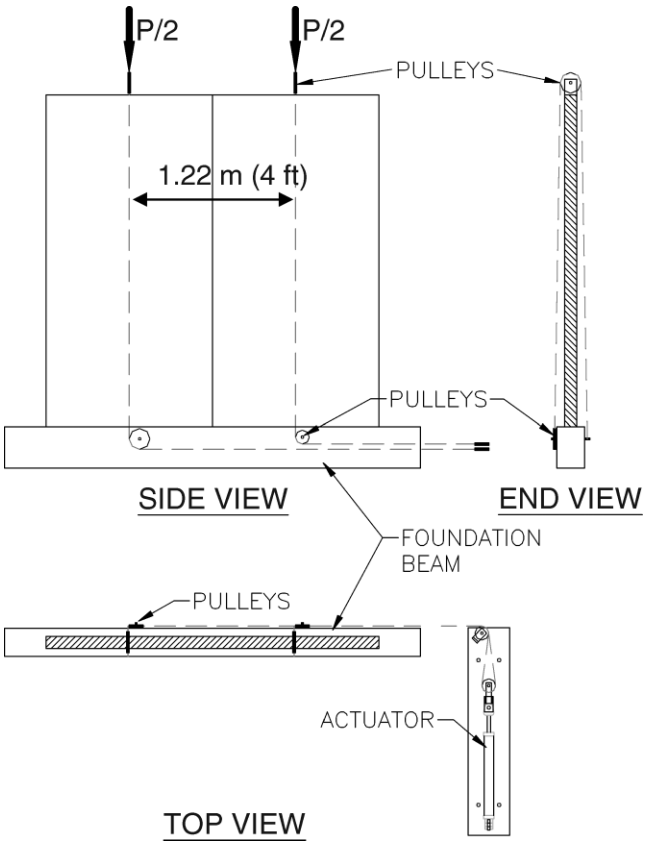

Figure 1.—Schematic of dead load assembly (Seaders 2004).

Two load cells were used to measure wall forces during testing. A 90-kN (20-kip) load cell was connected in-line with the hydraulic actuator and the steel beam serving as the foundation for the walls. This measured the force at the bottom of the wall to achieve the desired ground motion and move the seismic mass. The second load cell was 55.6-kN (12.5-kip) rated and in-line between the top of the steel moment arm and the steel channel bolted to the top of the wall, measuring force at the top of the wall. Load beam displacement was monitored by a sensor built into the hydraulic actuator measuring the cylinder position. Displacement at the top of the wall was monitored using a string potentiometer between the strong-wall and the double top plate. Uplift displacements of the double top plate with respect to the end stud of the wall, and the end stud with respect to the foundation, were also monitored. For the double top plate, this was achieved by mounting a linearly variable differential transducer (LVDT) on the end stud and monitoring its displacement with respect to the steel channel bolted to the top of the wall. Likewise, an LVDT was mounted on the end stud, and its displacement with respect to the foundation was monitored for bottom uplift. Uplift was recorded from one side of the wall only to ensure that a high-frequency data-sampling rate could be maintained (necessary to embody the dynamic response of the wall). If needed, the uplift response of the opposite end of the wall could be determined as function of drift and the measured uplift response. Data collection rate for all gauges was 50 Hz for dynamic testing.

Earthquake time histories

Selection.—Four ground motions, each from an individual historic earthquake, from the SAC Steel Project (SE03, SE07, SE13, and SE19; Somerville et al. 1997) were selected by White et al. (2009). Because the tests by White et al. did not incorporate gravity load, or a sequence of earthquake ground motions, the results provided a benchmark for the tests of the current study. The SE19 ground motion was the most severe and caused the most observed damage to both FA and PA walls (White et al. 2009), so it was selected for this study with gravity loads.

As for the earthquake ground motions, it was desired to subject walls first to an original, historical earthquake ground motion (i.e., a displacement time history that actually occurred) that would not cause total wall failure and then to an earthquake ground motion that had been used

previously in a single-test-only scenario. The second criterion would allow inferences to be drawn based on performance comparisons of nonsequence and sequence tests in this study. SE13 fulfilled these two requirements and was therefore selected for the earthquake ground motions test sequence.

Scaling.—Three earthquake ground motions were used in this study: (1) the SE19 ground motion scaled to the Seattle design level (10% probability of exceedance in 50 y) in tests where gravity load was applied to walls, (2) the unscaled SE13 ground motion for the first test of the earthquake ground motion sequence, and (3) the SE13 ground motion scaled to the Seattle design level (10% probability of exceedance in 50 y) in the second and final test of the earthquake ground motion sequence. Note that 10 percent probability of exceedance in 50 years is traditionally associated with life-safety performance.

Acceleration time histories were obtained from the SAC Steel Project. However, they had been scaled from the actual ground motion to match a design spectrum at periods of interest for steel structures. Because taller steel structures generally have a longer period of vibration than wood-frame structures, the time histories needed to be rescaled for this study. The procedure used to scale the time histories to the Seattle Design Level (10% probability of exceedance in 50 y) was the same as that described in White et al. (2009). Because the first test of the SE13 earthquake ground motion test sequence needed an unscaled ground motion, the scaled SE13 acceleration time history was rescaled to the original time history using the inverse of the ratio (or scale factor) that the SAC used.

Test matrix

Between Phase I (Seaders et al. 2009), Phase IIA (White et al. 2009), and Phase IIB (described here) of the project, 42 earthquake ground motion tests were conducted. Both phases consisted of two wall types (FA and PA) to determine performance differences with respect to testing protocol. Eight preliminary earthquake ground motion tests were conducted in Phase I although the primary focus was on monotonic and cyclic testing. Earthquake ground motion testing was the primary interest of Phase II, with 34 such tests (on 30 walls) conducted. White et al. (2009) reported the results of 20 of these ground motion tests. In Phase IIB, 14 earthquake ground motion tests on 10 walls are reported, as shown in Table 1. This preliminary study focuses on behavior rather than developing design values, thus the relatively small number of tests. Because Phase IIB included an earthquake ground motion test sequence, the first test in the sequence will be referred to as SE13-1 (unscaled), and the second test will be denoted SE13-2 (scaled to Seattle design level). Each wall specimen was subjected to both loading protocols. The results from the SE13 single earthquake ground motion tests of Seaders et al. (2009) will be referred to simply as SE13; these results were used to gauge the effect of the earthquake ground motion test sequence.

Table 1.—Test matrix.

Anchorage	SE19 with vertical load (1,090 kg [2,410 lb])	SE13 earthquake ground motion sequence[a]
PA	3	2
FA	3	2

[a] Composed of SE13-1 and SE13-2 tests.

Results and Discussion

Earthquake testing with dead load

Failure modes.—FA walls with dead load subjected to the SE19 ground motion exhibited a significant amount of damage. Damage primarily consisted of nails withdrawing from the frame along all of the panel edges; most intensively along the top plate, end studs, and sill plate. Along the center stud of the wall, the nails either tore through the edge of the panel or withdrew from the stud. About 25 percent of the screws along the end studs and center stud attaching the GWB to the frame fractured, while the remainder caused severe, localized crushing to the GWB. Screws along the top and bottom (sill) plates either caused severe, localized crushing or tearing at the edge of the panel, or both. Fasteners attaching the OSB or GWB sheathing to the frame along intermediate studs did not show signs of damage.

For PA walls tested with dead load, the primary damage occurred along the sill plate. Nails attaching the OSB to the frame along the sill plate tore through the edge of the OSB at the outer edges of the wall and at the inner corners of the panels. The other nails along the sill plate either withdrew or were pulled through the OSB sheathing. Additional damage included minor nail withdrawal along the top plate, end studs, and center stud. As for damage to the GWB, the screws attaching it to the frame along the top plate and end studs caused severe localized crushing of the GWB. Screws along the center stud mostly caused severe localized crushing of the GWB, though some tore through the edge of the panel. In addition, screws tore through the edge of the GWB panel along the entire length of the sill plate. No damage was observed around fasteners attaching the OSB or GWB to the frame along intermediate studs.

Overall, the damage patterns of FA walls with dead load were consistent with, but more severe than, those of tests without dead load (White et al. 2009). For PA walls with vertical load, the primary damage of edge breakout at fasteners along the sill plate was consistent with tests not containing vertical load in White et al. (2009). However, PA walls with dead load had additional damage, including a greater occurrence of nail withdrawal and localized crushing of the GWB along exterior framing members other than the sill plate. The other fastener failures exhibited during PA tests with dead load were common to FA tests with dead load. This provides evidence that vertical load resisted overturning forces imposed upon the wall, and it suggests that with respect to failure mode, PA and FA wall performances converge when vertical loads are applied.

Effect of dead load on performance.—Table 2 summarizes average performance parameters derived from backbone curves (Fig. 2) for SE19 earthquake ground motion tests with and without dead load. FA and PA wall tests with dead load are designated SE19-FA-DL and SE19-PA-DL, respectively. SE19 tests of FA and PA walls without dead load (White et al. 2009) are referred to as SE19-FA and SE19-PA, respectively. SE19-FA and SE19-PA tests provide a baseline for determining the effect that dead load has on wall performance under earthquake conditions.

With respect to maximum load (P_{max}), the SE19-FA-DL tests exhibited an 11 percent increase compared with the SE19-FA test, while the SE19-PA-DL test had a 110 percent

Table 2.—Selected parameters from SE19 earthquake ground motion tests with and without dead load.

Parameter	FA	FA-DL[a]	% diff.[b]	PA	PA-DL	% diff.
n	8	3	—	8	3	—
P_{max}, kN (kips)	21.43 (4.82)	23.72 (5.33)	11	8.34 (1.87)	17.52 (3.94)	110
Δ_{max}, mm (in.)	55.2 (2.17)	51.7	−6	20 (0.79)	60.8 (2.39)	204
E, J (ft-lb)	1,400 (1,030)	1,660 (1,220)	19	235 (173)	1,263 (930)	437
k_e, kN/mm (kips/in.)	1.55 (8.85)	1.67 (9.54)	8	1.07 (6.11)	1.18 (6.74)	10
μ	6.39	6.62	4	6.10	7.40	21

[a] DL = dead load.
[b] % diff. = percent difference between tests with DL and tests without DL.

increase in capacity compared with the SE19-PA test. As shown in Table 2 and Figure 2, the capacities of PA walls begin to approach that of FA walls when dead load is applied. This agrees with the damage patterns observed. In addition, these results also agree with monotonic tests from Ni and Karacabeyli (2002) and Seaders (2004) and the cyclic tests from Ni and Karacabeyli (2002).

For displacement at maximum load (Δ_{max}), the application of dead load on FA walls caused a slight (6%) decrease in value while causing a slight (8%) increase in wall stiffness (k_e). For PA walls, dead load application resulted in a 204 percent increase in Δ_{max} and a 110 percent increase in wall capacity.

With respect to energy dissipation (E), FA walls exhibited a 19 percent increase, while PA walls showed a 437 percent increase as a result of dead load application. Among the performance parameters, E had the largest relative change (gain or loss) as a result of dead load application. This is because PA walls with dead load were able to provide much larger loads and displacements.

FA walls exhibited a slight increase in k_e and ductility ($\mu = \Delta_{failure}/\Delta_{yield}$) with vertical load application. PA walls with vertical load also experienced the increases in k_e and μ, but these were modest compared with those of P_{max}, Δ_{max}, and E.

In general, PA walls reaped the most benefit from vertical loading. For FA walls, changes in measured and calculated parameters were modest in comparison to those for PA walls as a result of vertical loading. This is because PA wall performance is limited by the edge breakout capacity of the fasteners that attach the sheathing to the sill plate when dead load is absent. When dead load is present, this limitation still exists; however, dead load adds additional resistance to the overturning forces that cause the edge breakout to occur, thereby improving the wall performance.

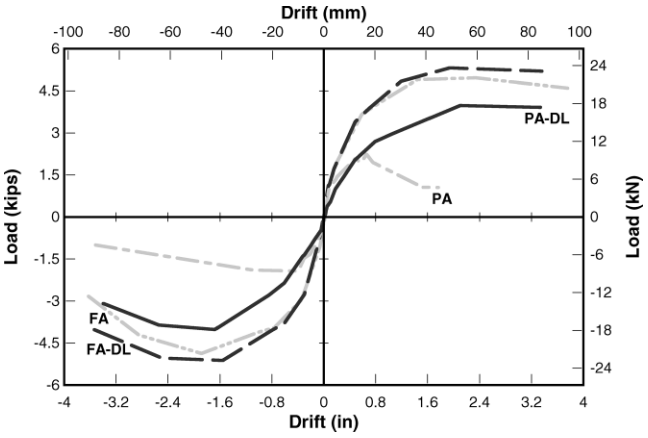

Figure 2.—Typical backbone curves for SE19 earthquake ground motion tests of fully and partially anchored walls with and without dead load.

Shear wall response resulting from a sequence of earthquake ground motion tests

Failure modes.—For FA walls, the SE13-1 test caused no visible damage. Most of the damage caused by the earthquake ground motion sequence came from the SE13-2 test. The SE13-2 test caused a few fasteners attaching the OSB to the sill plate to slightly withdraw from the framing. Additional damage included some minor nail withdrawal along the center stud and pull-through along the GWB edges that was most severe at the bottom of the wall. Overall, for FA walls, damage from the SE13 earthquake sequence (SE13-1 and SE13-2) seemed to be slightly less than that resulting from the single SE13 test. SE13-1 did not significantly load the wall and, thus, had very little effect on the overall performance of the wall during the SE13-2 test. Moreover, the walls had greater stiffness in the earthquake ground motion test sequence.

For PA walls, the SE13-1 test caused some minor nail withdrawal around the edges of the wall and some localized crushing of the GWB. Most damage to these walls resulted from SE13-2. Damage primarily occurred along the sill plate and involved the nail fasteners that attach the OSB to the frame withdrawing from the frame and tearing through the edge of the panel. Likewise, the screws attaching the GWB to the frame tore through the panel edge along the sill plate. Fastener damage along the sill plate was less severe in the middle of the wall and most severe along the outer edges of the wall. In both tests, some minor nail withdrawal from the frame occurred at the top plate, and in one test, the end studs pulled completely free from the sill plate and were resting on top of the nails driven through their end-grain to attach them to the sill plate. Most of the damage from the earthquake ground motion sequence resulted from SE13-2 for PA walls. In addition, total damage to PA walls resulting from the SE13 earthquake ground motion sequence was about the same as that from the single SE13 test. SE13-1 did not significantly load the wall and, thus, had very little effect on the overall performance of the wall during the SE13-2 test. In addition, the damage that PA walls can accumulate, and the wall capacities are limited by the edge breakout strength of the sheathing to sill plate fasteners (White et al. 2009).

Performance resulting from unscaled SE13 test.—Table 3 summarizes the average results of P_{max}, Δ_{max}, and E for FA and PA walls from the SE13-1 and SE13-2 tests. In addition,

Table 3.—Performance of FA and PA walls during the SE13 earthquake ground motion test sequence.

Parameter	FA			PA		
	SE13-1	SE1-2	Ratio[a]	SE13-1	SE13-2	Ratio
N	2	2	—	2	2	—
P_{max}, kN (kips)[b]	10.57 (2.37)	21.69 (4.88)	2.1	6.59 (1.48)	9.47 (2.13)	1.4
Δ_{max}, mm (in.)[b]	4.4 (0.17)	30.6 (1.20)	7.0	7.9 (0.31)	21.1 (0.83)	2.7
E, J (ft-lb)[b]	24.3 (17.9)	469 (346)	19.3	31.6 (23.3)	244 (180)	7.7
k_4, kN/mm (kips/in.)[c]	2.41 (13.8)	1.93 (11.0)	0.8	1.09 (6.22)	0.75 (4.28)	0.7
T_0, s[d]	0.273	0.305	1.1	0.406	0.489	1.2

[a] Ratio of SE13-2 values to SE13-1 values (SE13-2/SE13-1).
[b] Maximum observed values for SE13-1-FA, SE13-2-FA, and SE13-1-PA tests. Backbone curves did not reach ultimate load.
[c] Stiffness of backbone curve up to 4 mm (0.16 in.).
[d] k_4 was used in T_0 calculation.

Figure 3 depicts typical backbone curves for the SE13 test and for the SE13-1 and SE13-2 tests.

For FA walls, on average, SE13-2 caused loading about twice that measured during the SE13-1 test. For SE13-1, Δ_{max} and E were negligible in comparison to values from SE13-2. Moreover, an examination of Figure 3 for SE13-1 shows the FA wall backbone curve is linear; SE13-1 caused linear elastic response and did not damage FA walls.

For PA walls, SE13-2 caused loading that was 44 percent larger than that in the SE13-1 test. Both Δ_{max} and E levels from the SE13-1 test were much smaller than those from SE13-2. Figure 3 shows that the backbone curve from SE13-1 for PA walls is nonlinear, unlike that of FA walls. These results suggest that both FA and PA walls were not significantly affected by the first test of the SE13 earthquake ground motion sequence.

For both FA and PA walls, wall stiffnesses during the SE13-1 and SE13-2 tests were different. In this case, the slope of the backbone curve up to 4 mm (0.16 in.) of drift was used to determine stiffness, because the largest drift exhibited by FA walls during SE13-1 was approximately 4 mm (0.16 in.). During the SE13-2 test, FA and PA walls exhibited approximately 20 and 30 percent, respectively, lower stiffness (k_4) than during the corresponding SE13-1 test. The load cycling during the SE13-1 test ''loosened'' nails within their embedment locations and caused this reduction in stiffness.

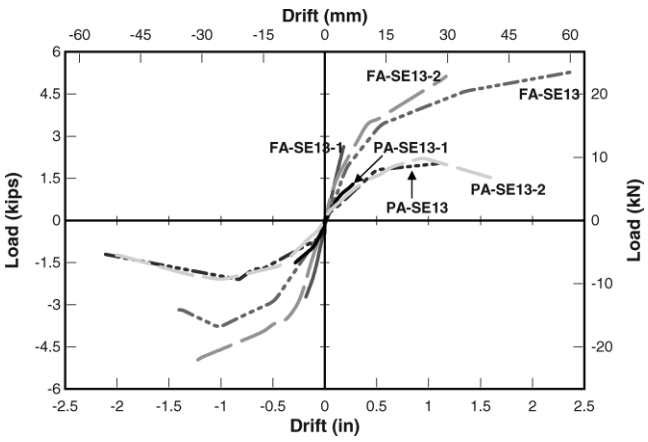

Figure 3.—Typical backbone curves of fully and partially anchored walls from SE13 sequence and nonsequence earthquake ground motion tests.

Lower wall stiffness during SE13-2 resulted in a longer fundamental period of vibration (T_0) when compared with the first test of the earthquake ground motion sequence. Fundamental periods of FA and PA walls were about 10 and 20 percent, respectively, larger during the second test of the earthquake sequence. This increase in wall period affects the wall's response to ground motion as reflected in the response spectrum.

Performance resulting from scaled SE13 test.—The FA wall SE13-2 test did not reach ultimate loading conditions; therefore, maximum observed values are reported for this test in Table 3. Although ultimate load did not occur as a result of SE13-2, Figure 3 shows that the FA SE13-2 test yielded a backbone curve that provides an upper bound to that of the FA SE13 test; however, it is not clear whether the backbone curve would have continued to provide an upper bound at drifts beyond those seen during the SE13-2 test. Nonetheless, this means that larger levels of wall strength, energy dissipation, and stiffness were achieved up to drifts of ±30 mm (1.2 in.) when walls were subjected to a sequence of SE13 earthquakes. Note that for as yet unexplained reasons, wall stiffness to 4 mm (k_4) during the second test of the SE13 earthquake sequence was approximately 38 percent greater than that of FA walls during the nonsequence SE13 test.

For PA walls, the backbone curves for SE13 and SE13-2 reveal that both tests resulted in ultimate and failure loading conditions, and that the shape of the backbone curves appears to be quite similar (Fig. 3). This suggests PA walls exhibited similar performance during these two tests.

With respect to P_{max}, SE13-2 test exhibited a P_{max} 8 percent larger than that of SE13. The SE19 tests of PA walls (White et al. 2009) had a larger sample size (eight walls) and exhibited a coefficient of variation (COV) for P_{max} of approximately 9 percent. Thus, the 8 percent difference in P_{max} from SE13 and SE13-2 appears to be within the variability associated with this parameter for earthquake tests because of the inherent nature of wood materials and construction practices.

Comparison of Δ_{max}, E, and k_4 from the PA SE13 and SE13-2 tests shows small differences and, therefore, suggests that PA walls had similar performance as a result of these tests. In addition, μ from the SE13-2 test was 24 percent smaller than that of the SE13 test. However, this difference is well within the 39 percent COV for μ from the PA SE19 tests (White et al. 2009). In addition, the 5 percent lower wall stiffness (k_4) during the SE13-2 test corresponded to an SE13 response spectrum acceleration of 0.86g that was only 8 percent lower than SE13 (0.93g). This also

suggests that PA wall response should be similar during the SE13 and SE13-2 tests and, therefore, parallel to results for P_{max}, Δ_{max}, E, k_4, μ, and backbone curves from these tests.

Overall, for PA walls, it appears likely that the SE13 test and the SE13-2 test exhibited similar performance as a result of (1) the inherent variability associated with wood materials and corresponding construction practices and/or (2) the SE13-1 test resulting in low levels of loading and causing very little damage to the wall.

Conclusions

Conclusions based on the results of this preliminary study include the following:

1. For PA walls with dead load, failure modes were consistent with tests without dead load; however, additional fastener damage common to FA walls resulted from the vertical load, providing additional resistance to overturning. In general, with respect to P_{max}, Δ_{max}, E, and μ, PA walls realized a greater improvement in performance than FA walls from dead load application. PA wall performance appears to converge with that of FA walls when dead load is applied.
2. PA walls tested with a sequence of SE13 ground motions exhibited performance with respect to wall capacity (P_{max}), deflection at maximum load (Δ_{max}), energy dissipation (E), and wall stiffness up to 4 mm (0.16 in.; k_4) that was about the same as that from the nonsequence SE13 test. It appears likely these results are caused by (1) SE13-1 low levels of loading and very little damage to the wall and/or (2) the typical variation in these parameters as a result of the inherent variability associated with wood materials and corresponding construction practices.

Literature Cited

Dujic, B. and R. Zarnic. 2001. Influence of Vertical Load on Lateral Resistance of Timber Framed Walls. Univ. of Ljubljana, Ljubljana, Slovenia.

Durham, J., M. He, F. Lam, and H. G. L. Prion. 1998. Seismic resistance of wood shear walls with oversize sheathing panels. *In:* Proceedings of the World Conference on Timber Engineering, August 17–20, 1998, Montreux, Switzerland; Presses Polytechniques et Universitaires Romandes, Montreux-Lausanne, Switzerland. Vol. 1:396–403.

Durham, J., F. Lam, and H. Prion. 2001. Seismic resistance of wood shear walls with large OSB panels. *ASCE J. Struct. Eng*. 127(12): 1460–1466.

He, M., F. Lam, and H. G. L. Prion. 1998. Influence of cyclic test protocols on performance of wood-based shear walls. *Can. J. Civil Eng*. 25(6):539–550.

International Code Council (ICC). 2006. International Residential Code. ICC, Whittier, California.

International Organization for Standardization (ISO). 1998. Timber structures—Joints made with mechanical fasteners—Quasi-static reversed-cyclic test method. WG7 Draft, ISO TC 165. ISO, Secretariat Standards Council of Canada, Ottawa.

Karacabeyli, E. and A. Ceccotti. 1996. Test results on the lateral resistance of nailed shear walls. *In:* Proceedings of the International Wood Engineering Conference, October 28–31, 1996, New Orleans, Louisiana. Vol. 2:179–186.

Karacabeyli, E. and A. Ceccotti. 1998. Nailed wood-frame shear walls for seismic loads: Test results and design considerations. Structural Engineering World Wide, Paper T207-6. Elsevier Science, New York.

McMullin, K. M. and D. S. Merrick. 2000. Seismic testing of light frame shear walls. Paper No. 5-4-1 presented at the Proceedings of the Sixth World Conference on Timber Engineering, July 31–August 3, 2000, Whistler, British Columbia, Canada. (CD-ROM.)

Ni, C. and E. Karacabeyli. 2002. Capacity of shear wall segments without hold-downs. *Wood Design Focus* 12(2):10–17.

Ni, C., E. Karacabeyli, and A. Ceccotti. 1999. Design of shear walls with openings under lateral and vertical loads. *In:* Proceedings of the Pacific Timber Engineering Conference, March 14–18, 1999, Rotorua, New Zealand. Vol. 1:110–117.

Pacific Northwest Seismographic Network. 2005. About us—The Pacific Northwest Seismographic Network. http://www.pnsn.org/INFO_GENERAL/INFOSHEET/welcome.html. Accessed January 20, 2005.

Portland Cement Association. 1997. Home builder report of 1997. Portland Cement Association, Skokie, Illinois.

Seaders, P. 2004. Performance of partially and fully anchored wood frame shear walls under monotonic, cyclic, and earthquake loads. Master's thesis. Oregon State University, Corvallis.

Seaders, P., T. H. Miller, and R. Gupta. 2009. Performance of partially and fully anchored wood-frame shear walls under earthquake loads. *Forest Prod. J*. 59(5):42–52.

Somerville, P., N. Smith, S. Punyamurthula, and J. Sun. 1997. Development of ground motion time histories for phase 2 of the FEMA/SAC Steel Project. Report No. SAC/BD-97/04. SAC Joint Venture for the Federal Emergency Management Agency, Washington, D.C.

White, K. B., T. H. Miller, and R. Gupta. 2009. Seismic performance testing of partially and fully anchored wood-frame shear walls. *Wood Fiber Sci*. 41(4):396–413.

Yanaga, K., Y. Sasaki, and T. Hirai. 2002. Estimation of shear resistance of nailed shear walls considering vertical loads and pull-up resistance of stud-bottom plate joints. *J. Wood Sci*. 48(3):152–159.